RESEARCH ARTICLE

Network-wise concordance of multimodal neuroimaging features across the Alzheimer's disease continuum

Jane Stocks[1] | Karteek Popuri[2] | Ashley Heywood[1] | Duygu Tosun[3] | Kate Alpert[1] | Mirza Faisal Beg[2] | Howard Rosen[3] | Lei Wang[1,4] | for the Alzheimer's Disease Neuroimaging Initiative[*]

[1]Department of Psychiatry and Behavioral Sciences, Feinberg School of Medicine, Northwestern University, Chicago, Illinois, USA

[2]School of Engineering Science, Simon Fraser University, Burnaby, British Columbia, Canada

[3]School of Medicine, University of California, San Francisco, California, USA

[4]Department of Psychiatry and Behavioral Health, Ohio State University Wexner Medical Center, Columbus, Ohio, USA

Correspondence
Jane Stocks, Department of Psychiatry and Behavioral Sciences, Feinberg School of Medicine, Northwestern University, 710 North Lake Shore Dr. #1318, Chicago, IL 60611, USA.
E-mail: janestocks2018@u.northwestern.edu

[*]Data used in preparation of this article were obtained from the Alzheimer's Disease Neuroimaging Initiative (ADNI) database (adni.loni.usc.edu). As such, the investigators within the ADNI contributed to the design and implementation of ADNI and/or provided data but did not participate in analysis or writing of this report. A complete listing of ADNI investigators can be found at:
http://adni.loni.usc.edu/wp-content/uploads/how_to_apply/ADNI_Acknowledgement_List.pdf

Abstract

Background: Concordance between cortical atrophy and cortical glucose hypometabolism within distributed brain networks was evaluated among cerebrospinal fluid (CSF) biomarker-defined amyloid/tau/neurodegeneration (A/T/N) groups.

Method: We computed correlations between cortical thickness and fluorodeoxyglucose metabolism within 12 functional brain networks. Differences among A/T/N groups (biomarker normal [BN], Alzheimer's disease [AD] continuum, suspected non-AD pathologic change [SNAP]) in network concordance and relationships to longitudinal change in cognition were assessed.

Results: Network-wise markers of concordance distinguish SNAP subjects from BN subjects within the posterior multimodal and language networks. AD-continuum subjects showed increased concordance in 9/12 networks assessed compared to BN subjects, as well as widespread atrophy and hypometabolism. Baseline network concordance was associated with longitudinal change in a composite memory variable in both SNAP and AD-continuum subjects.

Conclusions: Our novel study investigates the interrelationships between atrophy and hypometabolism across brain networks in A/T/N groups, helping disentangle the structure–function relationships that contribute to both clinical outcomes and diagnostic uncertainty in AD.

KEYWORDS
Alzheimer's disease, atrophy, biomarkers, concordance of atrophy and hypometabolism, concordance, fluorodeoxyglucose positron emission tomography, hypometabolism, magnetic resonance imaging, magnetic resonance imaging and fluorodeoxyglucose positron emission tomography concordance, multimodal neuroimaging, suspected non-Alzheimer's disease pathologic change, structure–function relationships

1 | INTRODUCTION

In sporadic Alzheimer's disease (AD), beginning years before clinical symptom onset, a cascade of pathophysiological changes occur involving the aggregation of amyloid beta (Aβ) and tau proteins leading to neurodegeneration.[1] An ongoing challenge in the study of AD is that of clinic-anatomical convergence, indicating the same clinical syndrome can be caused by different underlying pathological entities.[2] To this end, the "A/T/N" framework[3] has emphasized biomarkers as *ante mortem* predictors of AD pathology. Based on the presence/absence of markers of Aβ (A), phosphorylated tau (T), and neurodegeneration (N) in either the cerebrospinal fluid (CSF) or neuroimaging, the A/T/N classification schema results in three categories of biomarker abnormality: biomarker "normal" (BN; A–T–N–), "AD continuum" (any A+ category), and suspected "non-AD pathologic change" (i.e., SNAP, A– with either T+ or N+). Among these categories, SNAP has been proposed to represent a distinct pathological, clinical, and cognitive disease process from AD.[4,5] However, its cognitive profile, longitudinal trajectory, and *post mortem* pathology remain less well understood.

Structural magnetic resonance imaging (MRI) and positron emission tomography with ^{18}F-fluorodeoxyglucose (^{18}FDG-PET) have been used to measure brain atrophy and glucose hypometabolism, respectively. Multimodal analysis of anatomical and physiological change allows for the development of dynamic models of pathophysiological processes and can increase the power to characterize heterogeneity in clinical presentations of neurodegenerative disease processes.[6] Multimodal neuroimaging can measure the degree to which signals generated by each modality mirror the other in their strength, spatial distribution, or temporal ordering.[7] Termed "concordance," these markers have been used to directly compare patterns of brain atrophy and hypometabolism across different dementias.[8,9] Bejanin et al.[8] suggested that neurodegenerative disorders with a more unitary underlying pathophysiological disease process (i.e., semantic dementia due to TDP-43 Type C) may show higher concordance between hypometabolism and atrophy compared to a more multidetermined disease process (i.e., Aβ, tau in AD). However, prior studies measured concordance at the whole-brain or whole-lobe level, providing only a limited description of the link between structure and function in the brain. Given neurodegenerative diseases are hypothesized to spread along, and reflect damage to, large-scale brain networks spanning multiple regions,[1,10] network-based characterization of multimodal neuroimaging features can improve our understanding of the disease processes.

Studies have indicated that the neuroimaging patterns of cortical atrophy and glucose hypometabolism observed in AD continuum more closely resemble in vivo PET markers of tau than amyloid.[11] While SNAP individuals have positive markers of tau pathology on CSF, reported relationships between CSF phosphorylated tau (p-tau) and tau-PET has ranged from mild to strong and may vary by disease stage and the presence of amyloid.[12] Therefore, it is unclear whether structure–function concordance will occur in SNAP subjects, despite the observed relationship between tau and markers of neurodegeneration in AD.[11] This knowledge could aid in understanding

RESEARCH IN CONTEXT

1. **Systematic Review**: Concordance of fluorodeoxyglucose positron emission tomography and magnetic resonance imaging differentiate Alzheimer's disease (AD) from frontotemporal lobar dementia (FTLD), but prior work focused on whole-brain analyses, despite evidence that neurodegenerative disorders spread within circumscribed, selectively vulnerable brain networks. It remains unclear whether network-wise multimodal concordance can differentiate biomarker-normal individuals from AD continuum and suspected non-AD pathologic change (SNAP).

2. **Interpretation**: Findings support evidence that SNAP is a heterogeneous group regarding etiology; however, network-wise multimodal indicators of neurodegeneration are superior for distinguishing SNAP from biomarker normal subjects and for association with longitudinal change in memory.

3. **Future Directions**: Future research should examine whether increased concordance within the select networks represents a potential biomarker of neuropathologic change among SNAP individuals who progress to an FTLD syndrome. Further, future work could also examine those who are only amyloid positive (e.g., A+T–N–) as a distinct group or use data-driven measures of concordance (e.g., canonical correlation) for additional computational power.

the causes of neurodegeneration among this understudied group and provide information to allow treatment development that is tailored to the pathophysiology of the disease. Here, we computed maps of concordance between cortical atrophy and hypometabolism across the brain's functional networks for each individual, compared across A/T/N groups, and related them to longitudinal cognitive changes. We hypothesized that concordance would uniquely discriminate the A/T/N groups and be more sensitive than unimodal measures to future cognitive decline.

2 | MATERIAL AND METHODS

2.1 | Participants

Data were obtained from the Alzheimer's Disease Neuroimaging Initiative (ADNI) database. ADNI was launched in 2003 as a public–private partnership, led by principal investigator Michael W. Weiner, MD. The primary goal of ADNI is to test whether serial MRI, PET, other biological markers, and clinical and neuropsychological assessment can be used to understand disease progression in mild cognitive impairment

(MCI) and AD. Full details of participant recruitment, scanning protocols, diagnostic criteria, as well as imaging and CSF data processing are available at www.adni-info.org. ADNI protocols can be found in Jack et al.[13] and Mueller et al.[14] For this study, we included participants who had baseline CSF, structural MRI and [18]FDG-PET data, and neuropsychological testing data at both baseline and 12-month follow-up visits, to measure cognitive change. Twelve months was selected as a follow-up interval to retain the maximum number of participants and to allow sufficient time for cognitive change.

CSF samples were analyzed at the University of Pennsylvania, according to procedures and recommendations in the ADNI procedures manual, using Elecsys CSF immunoassays. Elecsys assays are fully automated, run on the Cobas e 601 analyzer (Roche Diagnostics GmbH) and have been reported to avoid the observed interlaboratory variation and upward drift of $A\beta42$ values seen in enzyme-linked immunosorbent assays.[15] Based on CSF measures of $A\beta1$-42, phosphorylated tau 181 (p-tau), and total tau (t-tau), we first designated A/T/N positivity using published cut-off points:[16] $A\beta1$-42 < 977 pg/mL for A+/A−, p-tau > 23 pg/ml for T+/T−, and t-tau > 213 pg/ml for N+/N−. We then designated the participants into the following A/T/N groups: BN (participants who were A−T−N−), AD continuum (amyloid-positive, i.e., A+T−N−, A+T−N+, A+T+N−, A+T+N+), or SNAP (the remaining amyloid-negative, i.e., A−T−N+, A−T+N−, A−T+N+).

2.2 | Image processing

2.2.1 | Structural MRI

ADNI MRI preprocessing included correction of geometric distortion, non-uniformity normalization, and histogram-peak sharpening. We processed all preprocessed MRI data with FreeSurfer v5.3[17] to generate cortical thickness measures with quality control by visual inspection. Erroneous segmentations were corrected according to FreeSurfer protocol. Sixteen scans were removed from further analysis due to large or immutable errors (Figure S1 in supporting information). Fourteen mm full width half maximum (FWHM) kernel was applied to the cortical thickness data along the cortical surface.[18] The cortical thickness data were then mapped onto the fsaverage template surface.

2.2.2 | [18]FDG-PET

Detailed ADNI preprocessing for [18]FDG-PET included co-registration, averaging, standardizing spatial resolution, orientation and normalization, and scanner-specific smoothing to achieve a uniform smoothing level of isotropic 8 mm FWHM. We co-registered all preprocessed [18]FDG-PET data with their respective MRI images using FSL-FLIRT,[19] using nine degrees of freedom and normalized correlation as the cost function. Cortical [18]FDG-PET uptake values were then re-indexed to the fsaverage template white surface and smoothed with a Gaussian smoothing kernel of 14 mm FWHM to achieve the same effective smoothness as the cortical thickness data.[20]

2.2.3 | W-score maps

The above MRI and [18]FDG-PET processing resulted in multimodal vectors of cortical thickness and [18]FDG-PET uptake, correspondingly indexed over the fsaverage template surface and smoothed to the same degree across all participants. Next, we computed vertex-wise W-scores[21] for cortical thickness and [18]FDG-PET uptake to adjust for the effects of normal aging (Figure 1A). W-scores were calculated by fitting a general linear model (GLM) against age in a set of reference participants, and taking the standardized residuals generated from this model for all participants:[22] W = ([raw value] − [expected value])/(standard deviation of the residuals of reference). For the reference set, we used cognitively normal individuals without a clinical diagnosis who do not progress to MCI or AD throughout the ADNI period (see Popuri et al.[23]). In our sample, the reference set comprised 423 subjects, 53% female, with a mean age of 74.4 (5.95).

2.3 | Analyses

2.3.1 | Participants

Differences in demographic and clinical variables across the A/T/N groups were assessed with two-way analysis of variance (ANOVA) for continuous data and Chi-square testing for categorical data, with post hoc comparisons wherever relevant. See Table 1.

2.3.2 | Network-wise unimodal atrophy, hypometabolism, and multimodal concordance

Using the Human Connectome Project-MMP1 atlas[24] that is based on multimodal features including cytoarchitecture and functional connectivity, the fsaverage template surface was parcellated into 360 patches corresponding to select cortical vertices (Figure 1A). These patches have been grouped into 12 functional networks by Ji et al.[25] via a community detection algorithm using resting-state data from healthy adults.

For unimodal analysis, the mean W-scores of cortical thickness and [18]FDG-PET uptake within each network were calculated. Each network-wise unimodal measure of cortical thickness and [18]FDG-PET uptake was entered into a separate GLM with A/T/N group as the main effect and sex, apolipoprotein E (APOE) ε4 status, Clinical Dementia Rating scale Sum of Boxes (CDR-SB),[26] and education as covariates. Post hoc tests contrasted AD continuum and SNAP groups with BN. For each group pair, this produced a coefficient estimate and pooled standard error for group, from which a t-statistic was calculated and visualized as a color map on the overall average surface. In these and all subsequent analyses described below, significance levels were corrected for multiple comparisons by applying a false discovery rate (FDR) of 0.05.

For multimodal analysis, a concordance measure was calculated for each individual as the Pearson correlation coefficient between
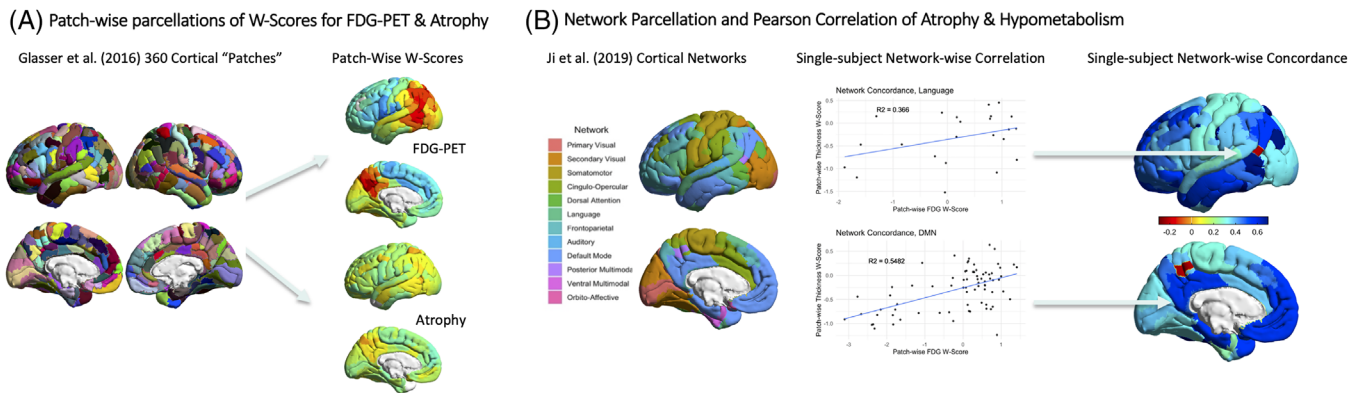
(A) Patch-wise parcellations of W-Scores for FDG-PET & Atrophy

(B) Network Parcellation and Pearson Correlation of Atrophy & Hypometabolism

FIGURE 1 Sample participant to demonstrate methods used for the network concordance analyses. A, Within each individual, vertex-wise magnetic resonance imaging (MRI) and fluorodeoxyglucose positron emission tomography (FDG-PET) W-Scores were parcellated into 360 cortical patches, and in (B) Pearson correlations between FDG-PET hypometabolism were computed per participant across the patches in each of 12 functional networks defined by Ji et al.[25]

TABLE 1 Table showing summary of demographic variables

	BN	SNAP	AD continuum	P	Post hoc test (P)		
	n: 179	n: 149	n: 559		AD-C vs. BN	SNAP vs. BN	AD-C vs. SNAP
Age	71.22 (7.5)	73.51 (6.8)	73.61 (6.8)	< **.001**	< **.001**	0.005	–
Male: Female	88:91	70:79	239:320	–	–	–	–
Education	16.3 (2.6)	16.2 (2.6)	16.0 (3.1)	–	–	–	–
CDR-SB	0.63 (0.8)	0.94 (1.3)	2.0 (1.9)	< **.001**	< .001		< .001
APOE ε4 Y: N	31:148	38:111	346:213	< .001	< .001	–	–
MMSE	24–30 (1.4)	21–30 (1.9)	19–30 (2.8)	< .001	< .001	–	< .001
ADNI-Mem	0.92 (0.7)	0.65 (0.7)	–0.058 (0.9)	< .001	< .001	0.003	< .001
ADNI-EF	0.82 (0.8)	0.67 (1.0)	–0.14 (1.3)	< .001	< .001	–	< .001
ATN subgroups	179 A–T–N–	102 A–T+N+	355 A+T+N+				
		47 A–T–N+	179 A+T–N–				
			25 A+T–N+				
			3 A+T+N–				
Clinical diagnosis (CN/MCI/dementia)	96/79/4	67/71/11	95/303/161	< .001			
Aβ pg/ml	1551 (316)	1943 (575)	675 (201)	< .001	< .001	< .001	< .001
P-tau pg/ml	15.9 (2.8)	28.9 (10.1)	31.5 (15.9)	< .001	< .001	< .001	–
T-tau pg/ml	183 (30.1)	322 (97.6)	315 (144)	< .001	< .001	< .001	–
	n: 167	n: 139	n: 510				
ADNI-Mem annual rate of change	0.013[a] (0.01)	–0.002 (0.01)	–0.035[a] (0.01)	< .001	< .001	–	0.005
ADNI-EF annual rate of change	0.02[a] (0.1)	0.05[a] (0.08)	0.003 (0.2)	0.007	–	–	0.009

Notes: Results are reported as mean (std) for continuous variables or counts for discrete variables, and *t*-statistic and *P*-value for post hoc pairwise analyses compared to BN subjects where ANOVA was significant. Age and education are reported in years. N's for ADNI-Mem and ADNI-EF annual rate of change reflect subjects with data for both baseline and 1-year assessments of neuropsychological function.

[a] For ADNI-Mem and ADNI-EF annual rate of change reflect significance in the direction change.

Abbreviations: Aβ, amyloid beta; AD, Alzheimer's disease; AD-C, Alzheimer's disease continuum; ADNI-EF, Alzheimer's Disease Neuroimaging Initiative Executive Functioning Composite; ADNI-Mem, Alzheimer's Disease Neuroimaging Initiative Memory Composite; ANOVA, analysis of variance; *APOE*, apolipoprotein E; BN, biomarker normal; CDR-SB, Clinical Dementia Rating–Sum of Boxes; CN, cognitively normal ; MCI, mild cognitive impairment; MMSE, Mini Mental State Examination; p-tau, phosphorylated tau; SNAP, suspected non-Alzheimer's disease pathologic change; t-tau, total tau.

patch-wise W-scores of cortical thickness and ^{18}FDG-PET uptake for each network (Figure 1B). The main effect of A/T/N group and contrasts between AD continuum, SNAP, and BN groups on multimodal network concordance were examined across all networks in the same manner as for the unimodal measures described above. Analyses were performed using the MATLAB 2018b[27] package SurfStat (http://www.math.mcgill.ca/keith/surfstat).[28]

2.3.3 | Network concordance by cognitive screening measure

Clinical heterogeneity exists within the A/T/N groups. Some individuals in AD continuum and SNAP may carry amyloid and tau pathologies but exhibit normal levels of cognition (see Table 1 Mini Mental State Examination [MMSE] range). The MMSE score of 26 has been shown to be an optimal threshold for dementia screening with 72% sensitivity and 94% specificity.[29] We therefore used this threshold to examine network concordance in cognitively impaired (CI) and cognitively unimpaired (CU) AD continuum and SNAP groups compared to unimpaired BN individuals using a GLM with age, sex, *APOE ε4* status, CDR-SB, and education as covariates.

2.3.4 | Relationship to cognitive change

Cognition was assessed for each individual using composite scales for memory and executive function (i.e., ADNI-Mem[30] and ADNI-EF,[31] respectively), calculated based on the ADNI neuropsychological battery. We calculated an annual rate of change for ADNI-Mem and ADNI-EF using linear mixed effects models. Age, sex, education, CDR-SB, and *APOE ε4* status were used as fixed effects, and random slope and intercept were used for time. Differences in annual rates of change in ADNI-Mem and ADNI-EF between groups were evaluated using two-sample *t*-tests. Rates of change were then regressed against network concordance across all networks with age, sex, education, *APOE ε4* status, and CDR-SB as covariates. To assess the contribution of concordance beyond unimodal atrophy and hypometabolism alone, the mean W-score of atrophy and hypometabolism were included as covariates. Analyses were performed using R[32] with the nlme package.[33]

3 | RESULTS

3.1 | Participants

At baseline, AD continuum (N = 559) and SNAP (N = 149) were older than BN (N = 179) (*P*<.05). AD continuum showed the greatest frequency of *APOE ε4* carriers (*P*<.001). MMSE, ADNI-Mem, ADNI-EF, and 1-year rate of change of ADNI-Mem were lower in AD continuum compared to BN (all *P*<.001). Baseline ADNI-Mem was lower in SNAP compared to BN (*P*<.01). No significant differences were detected between SNAP and BN on baseline ADNI-EF, ADNI-Mem rate of change, or

ADNI-EF rate of change. As expected, CSF measures of Aβ were lower while p-tau and t-tau values were greater in AD continuum than in BN (all *P*<.001). P-tau and t-tau values were greater, as expected, in SNAP than in BN (all *P*<.001); however, CSF Aβ values were greater in SNAP than BN (*P*<.001). See Table 1.

3.2 | Network-wise patterns of cortical atrophy, hypometabolism, and concordance among A/T/N groups

Figure 2 displays the W-score maps of cortical atrophy, hypometabolism, and concordance in each A/T/N group. Figure 3 displays comparisons of hypometabolism, atrophy, and concordance in AD continuum and SNAP versus BN. While SNAP showed no network-wise differences from BN in atrophy or hypometabolism, they showed greater atrophy–hypometabolism concordance in the language and posterior multimodal networks. AD continuum showed widespread hypometabolism affecting all networks except the somatomotor, primary and secondary visual networks, and cortical atrophy in all but the somatomotor and primary visual networks. AD continuum also showed increased concordance among secondary visual, somatomotor, cingulo-opercular, dorsal attention, language, auditory, frontoparietal, default mode, posterior and ventral multimodal networks. Regarding effects of covariates, *APOE ε4* positivity resulted in increased FDG-PET hypometabolism in all three groups among the secondary visual, dorsal attention, and ventral multimodal networks. No other significant effects of included covariates were noted.

Figure 4 shows comparisons of hypometabolism, atrophy, and concordance in AD continuum and SNAP versus BN after additionally controlling for clinical severity as measured by CDR-SB. Significant effects of CDR-SB were seen across all modalities, groups, and networks. In this model, SNAP showed no significant differences from BN in atrophy or hypometabolism but showed greater network concordance in the language and posterior multimodal networks. AD continuum showed greater hypometabolism in the frontoparietal, default mode, and posterior multimodal networks, and greater cortical atrophy in the ventral multimodal network only. AD continuum showed increased concordance among all except the primary visual and orbito-affective networks. Previously noted observed effects of *APOE ε4* positivity remained significant in the analyses controlling for CDR-SB. Significant differences between AD continuum and SNAP groups in unimodal and concordance measures, with and without CDR-SB included as a covariate, can be found in Figure S2 in supporting information.

3.3 | Network-wise concordance stratified by cognitive screening impairment

Figure 5 displays comparisons of network-wise concordance in CU and CI AD continuum and SNAP versus BN (BN-unimpaired, n = 158). The CI SNAP (SNAP-CI, n = 28) showed significantly greater concordance than BN-unimpaired in the dorsal attention, language, frontoparietal,
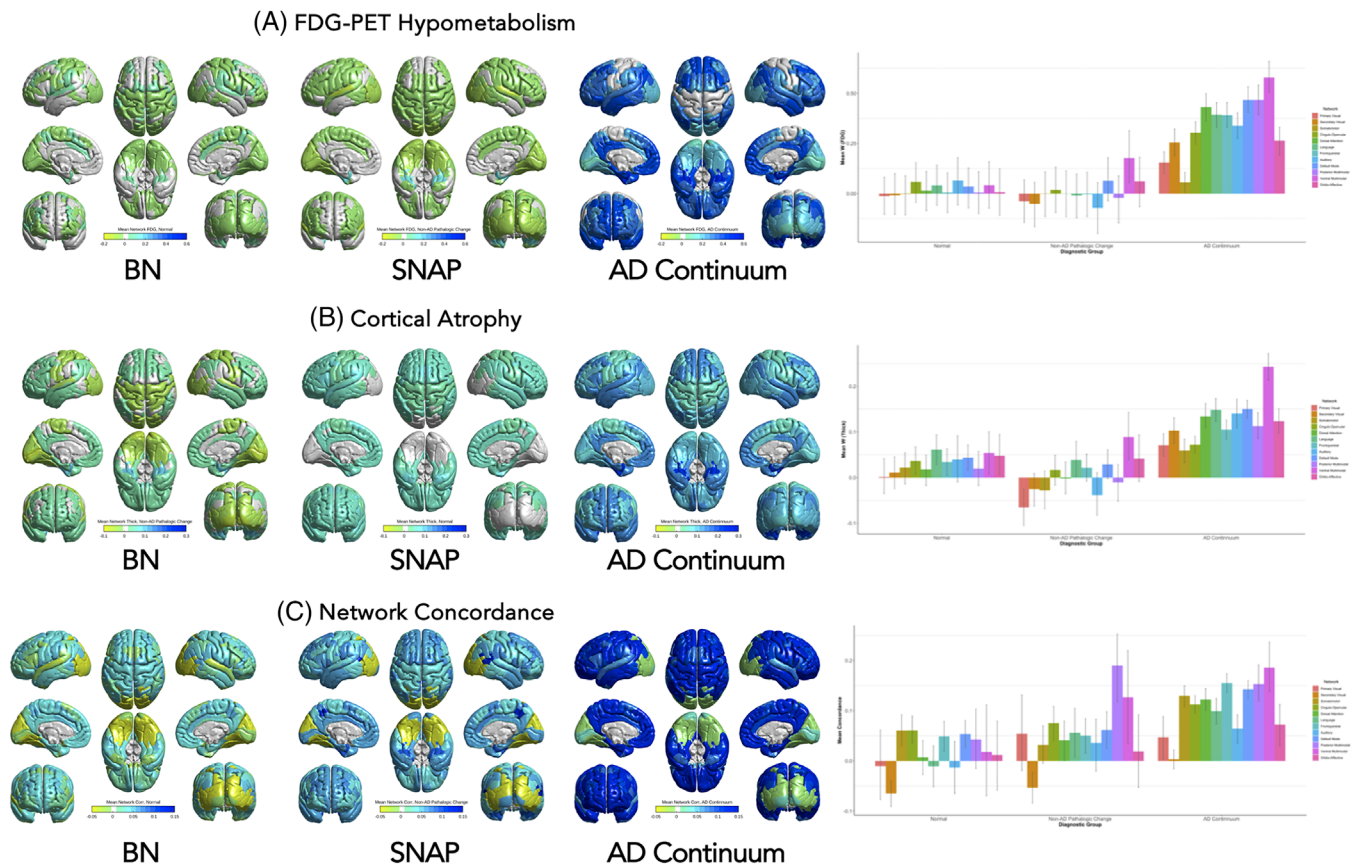
FIGURE 2 Within-group means of network-wise fluorodeoxyglucose positron emission tomography (FDG-PET) hypometabolism (A), cortical atrophy (B), and concordance (C) among ATN subgroups, displayed on the brain (left images) and in graphical format (right). Alterations within biomarker normal (BN; N = 179), suspected non-Alzheimer's disease pathologic change (SNAP; N = 149), and Alzheimer's disease continuum (N = 559) are expressed as mean W-score within each network for FDG-PET and atrophy, and mean Pearson correlation for concordance

default mode, and ventral multimodal networks. CU SNAP (SNAP-CU, n = 121) showed increased concordance compared to BN-unimpaired in the posterior multimodal network only. CI AD continuum (ADC-CI, n = 304) revealed significantly greater concordance than BN-unimpaired in all but the primary visual network. CU AD continuum (ADC-CU, n = 255) showed significantly greater concordance in the secondary visual, dorsal attention, language, frontoparietal, and default mode networks than BN-unimpaired.

3.4 | Relationship of network concordance to cognitive change

Among SNAP, increased concordance in the language network at baseline was associated with greater rate of decline in ADNI-Mem (Figure 6, top left). In AD continuum, greater baseline concordance in the primary visual, somatomotor, dorsal attention, language, frontoparietal, auditory, default mode, and orbito-affective networks were associated with greater rates of decline in ADNI-Mem (Figure 6, top right), and greater concordance in the secondary visual, dorsal attention, frontoparietal, and auditory networks were associated with greater rates of decline in ADNI-EF (Figure 6, bottom right). No relationships were found among

BN. Regarding effects of covariates on cognitive change, *APOE ε*4 positivity negatively impacted rate of ADNI-Mem decline among the AD continuum group only.

4 | DISCUSSION

We present the first study to investigate network-wise concordance of cortical atrophy and glucose hypometabolism, derived from structural MRI and [18]FDG-PET, respectively, among A/T/N biomarker groups. Results revealed that compared to BN, concordance was significantly increased in AD continuum across all except the primary visual and orbito-affective networks, and SNAP showed greater concordance in the language and posterior multimodal networks. These differences remained statistically significant after accounting for clinical disease severity.

Atrophy and [18]FDG-PET hypometabolism may reflect distinct yet complementary neurodegenerative processes.[34] Studies show that they each uniquely contribute to cognitive decline but also overlap in critical "hub" regions of functional networks.[35] In these regions, amyloid and tau may promote their synergistic deleterious effects[36] and "hub"-based connectivity models have been found to be predictive
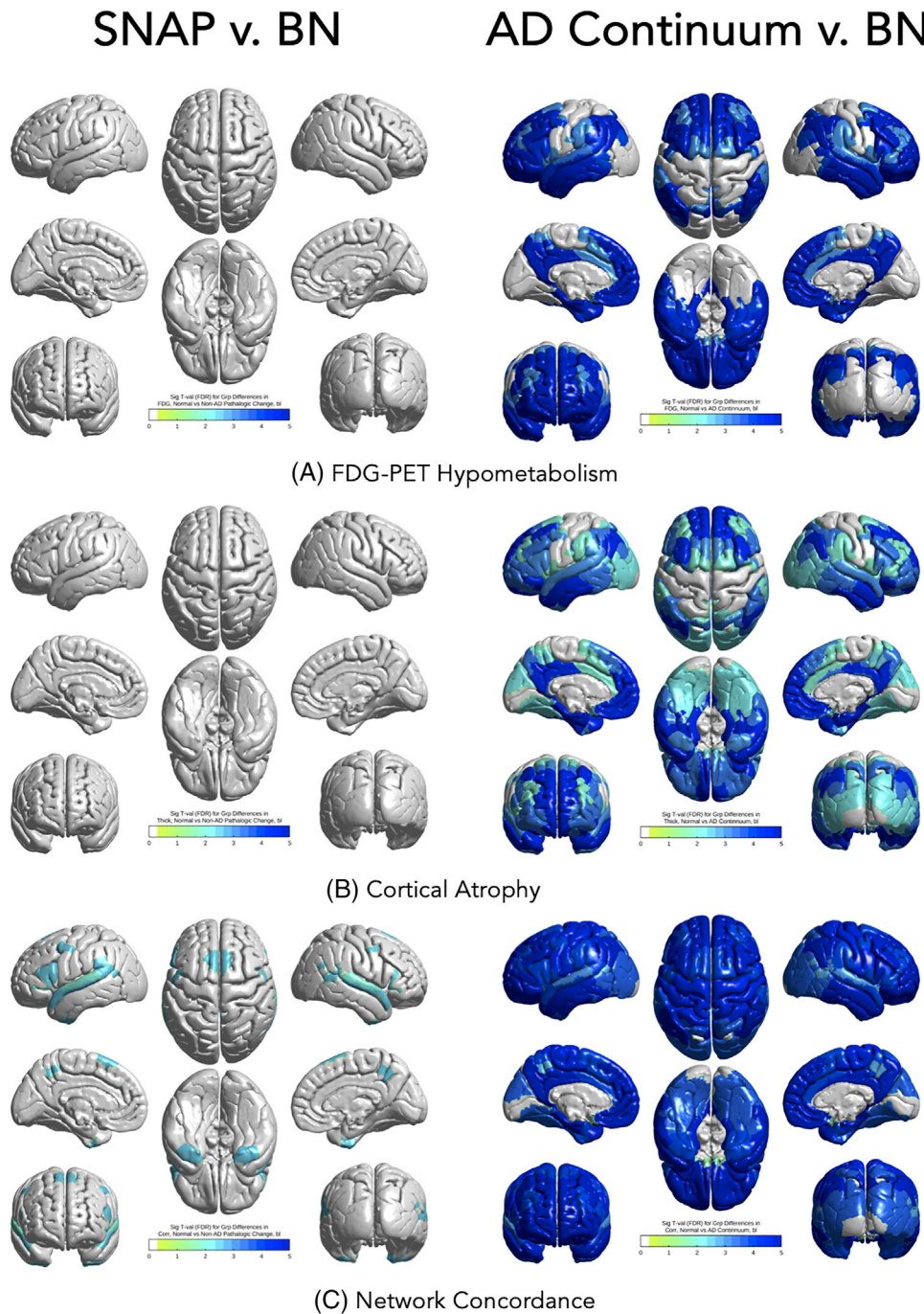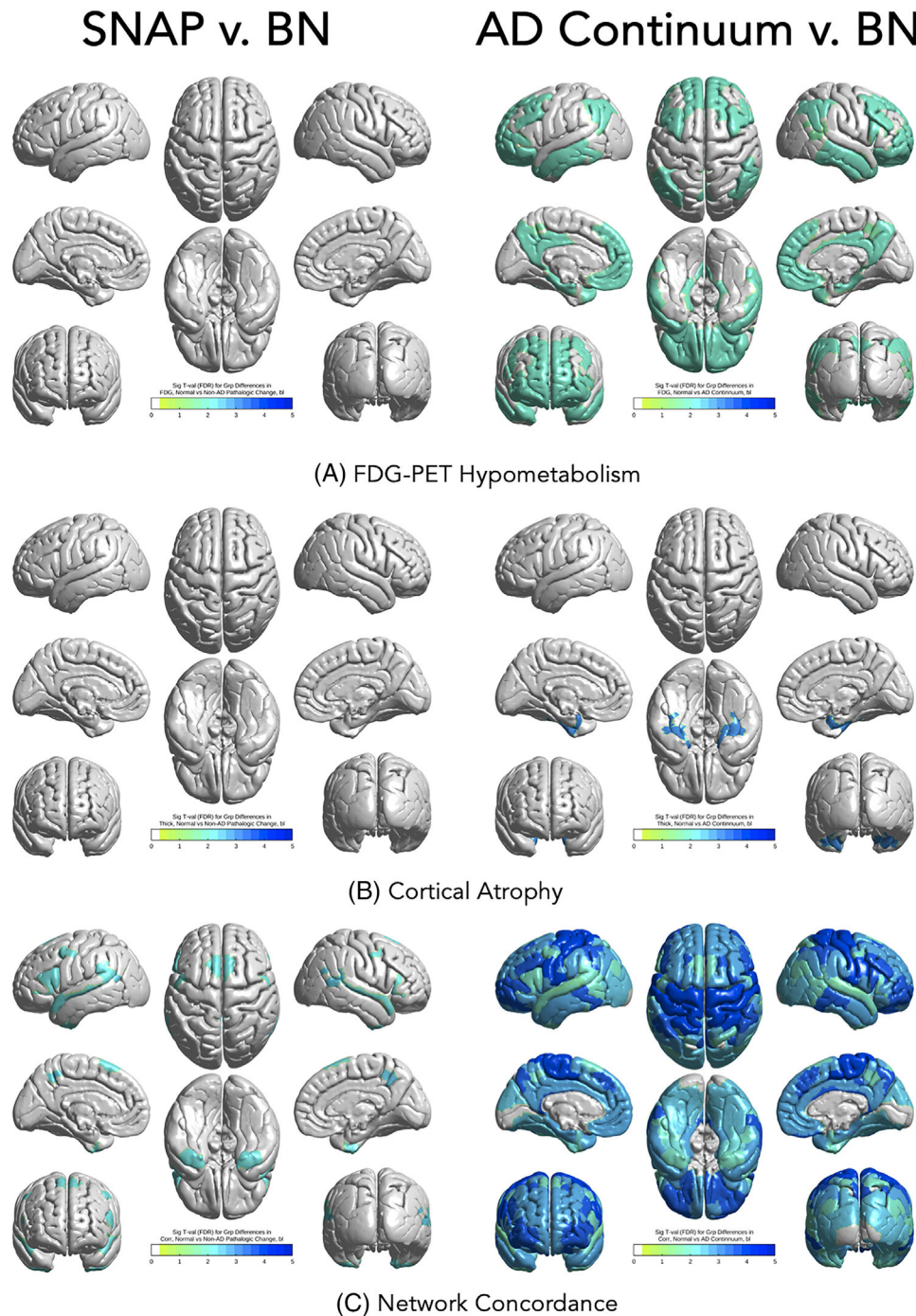
FIGURE 3 T-scores of false discovery rate–corrected significant networks in suspected non-Alzheimer's disease pathologic change (SNAP; N = 149) and Alzheimer's disease (AD) continuum (N = 559) groups compared to biomarker normal (BN; N = 179) participants in W-score transformed cortical thickness (top panel), W-score transformed fluorodeoxyglucose positron emission tomography (FDG-PET) hypometabolism (middle panel), and network concordance (bottom panel) after controlling for sex, education, apolipoprotein E ε4. SNAP showed no significant differences from BN in atrophy or hypometabolism after multiple comparisons correction. SNAP showed increased network concordance compared to BN in the language and posterior multimodal networks. AD continuum showed widespread hypometabolism in all but somatomotor, primary and secondary visual networks and significantly increased atrophy in all but somatomotor and primary visual networks. AD continuum showed increased concordance among secondary visual, somatomotor, cingulo-opercular, dorsal attention, language, auditory, frontoparietal, default mode, posterior, and ventral multimodal networks
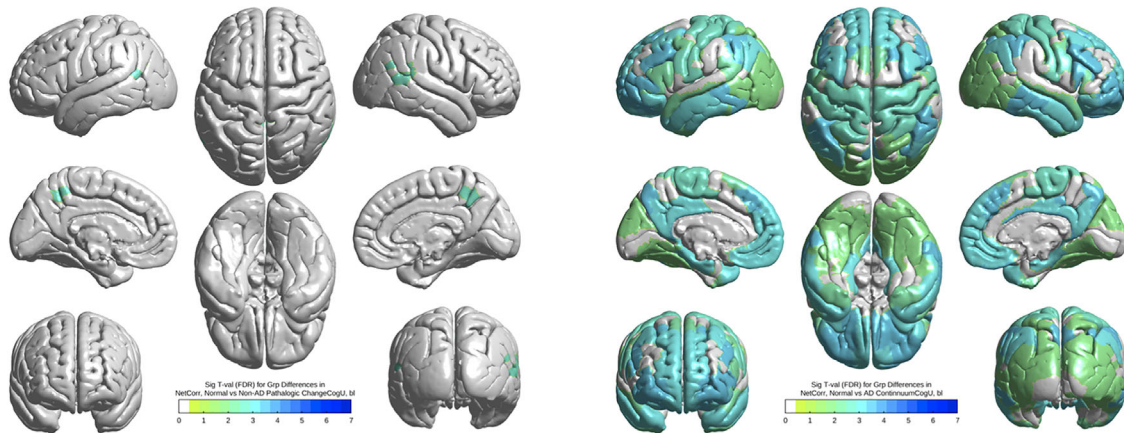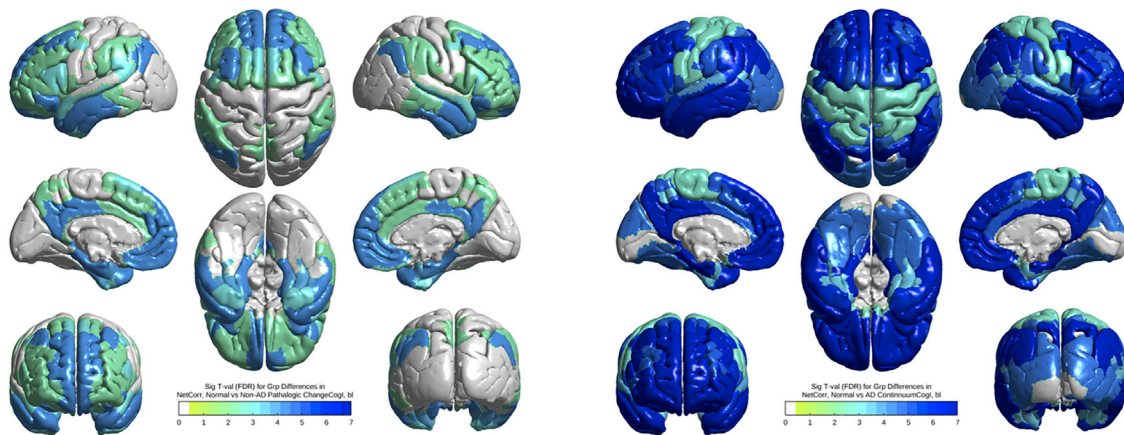
FIGURE 4 T-scores of false discovery rate–corrected significant networks in suspected non-Alzheimer's disease pathologic change (SNAP; N = 149) and Alzheimer's disease (AD) continuum (N = 559) groups compared to biomarker normal (BN; N = 179) in W-score transformed cortical thickness (top panel), fluorodeoxyglucose positron emission tomography (FDG-PET) hypometabolism (middle panel), and network concordance (bottom panel) after controlling for sex, education, apolipoprotein E ε4, and Clinical Dementia Rating-Sum of Boxes. SNAP showed no significant differences from BN in atrophy or hypometabolism. SNAP showed increased network concordance compared to BN in the posterior multimodal and language networks. AD continuum showed hypometabolism in all but somatomotor networks and significantly increased atrophy in all but somatomotor and cingulo-opercular networks. AD continuum showed increased concordance among secondary visual, somatomotor, cingulo-opercular, dorsal attention, language, auditory, frontoparietal, default mode, posterior, and ventral multimodal networks

FIGURE 5 Left panel, T-scores of false discovery rate (FDR)–corrected significant networks of suspected non-Alzheimer's disease pathologic change cognitively unimpaired (SNAP-CU; N = 121) and cognitively impaired (SNAP-CI, N = 28) SNAP subjects compared to cognitively unimpaired biomarker normal (BN; N = 158) subjects. Right panel, T-scores of FDR-corrected significant networks between cognitively unimpaired (ADC-CU, N = 255) and cognitively impaired (ADC-CI, N = 304) AD continuum subjects compared to BN subjects

of longitudinal atrophy in AD[37] and frontotemporal lobar degeneration (FTLD) syndromes.[38] These hubs have been proposed within the default mode and frontoparietal cognitive control networks for AD,[39] which in the present study showed strong concordance for AD continuum. We also found a high degree of atrophy–hypometabolism concordance in SNAP in the posterior multimodal network. The dorsomedial parietal and posterior cingulate regions of this network connect directly with the medial temporal areas that are vulnerable to tau.[40] This suggests that atrophy–hypometabolism synchrony may be a marker of particular vulnerability to tau pathology among SNAP.

Our unimodal analyses showed the expected widespread atrophy and hypometabolism in AD continuum, but little or no increased atrophy or hypometabolism in SNAP. This is consistent with prior research when SNAP was defined by abnormality in CSF p-tau and t-tau.[41] We also showed that SNAP exhibited mild declines on MMSE and memory compared to BN and increased atrophy–hypometabolism concordance in 2 out of 12 networks. Together, these results suggest that SNAP as defined by CSF may represent an early stage of the disease, in which evidence of pathological effects are measurable only in the CSF but not yet robustly in unimodal neuroimaging. Our results support the hypothesis that CSF-positivity of tau and neurodegeneration markers is likely an early marker along the pathological process leading to SNAP, and concordance markers are superior to unimodal imaging for differentiating from BN at this early stage.

Our results showed robust increases in network concordance for AD continuum and only in circumscribed networks for SNAP. The etiology of this difference is likely multi-determined. First, AD continuum represent a group with greater disease burden than SNAP, as evidenced by their cognitive and clinical severity scores and unimodal neuroimaging findings in the present study. Second, SNAP is
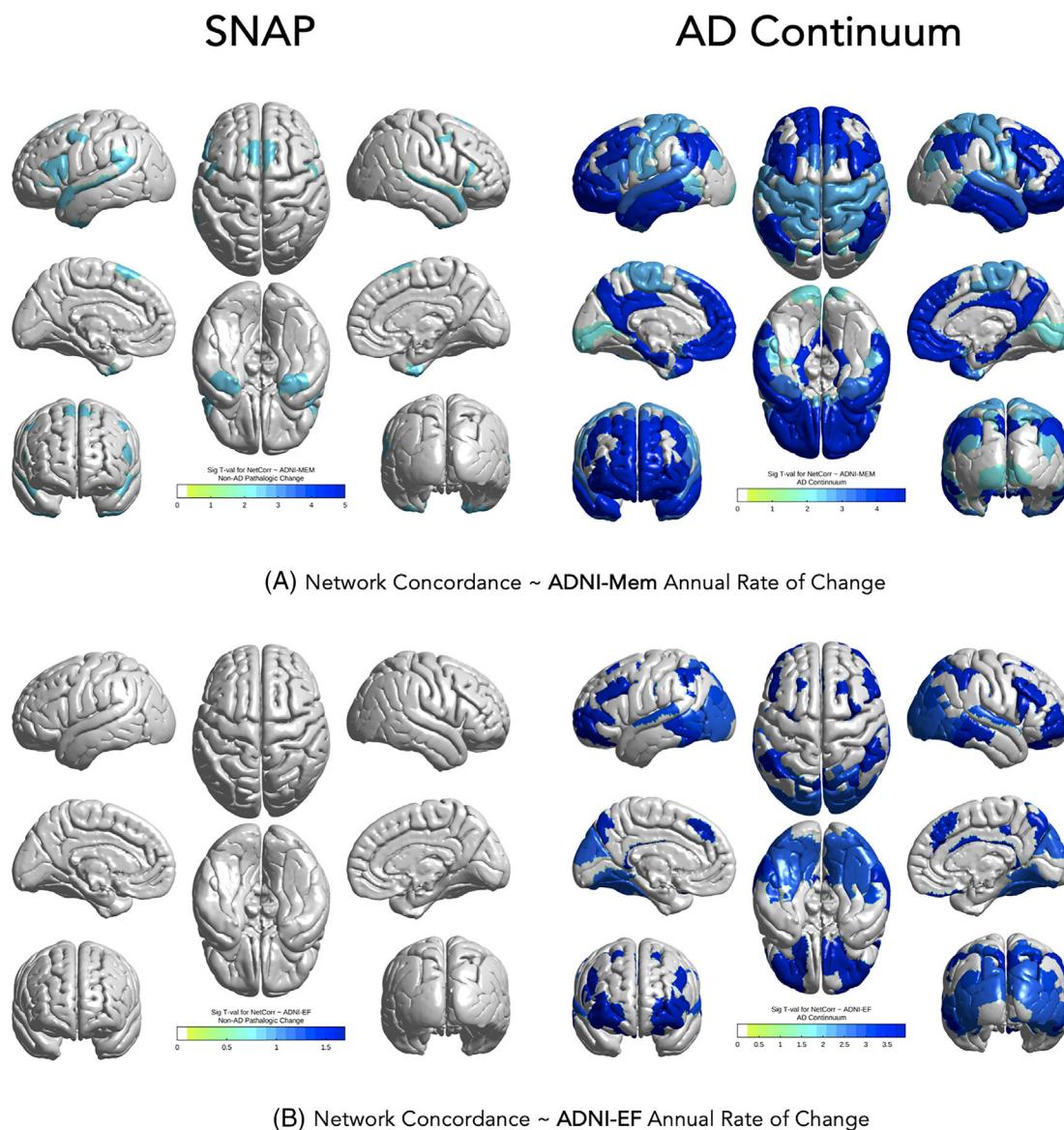
(A) Network Concordance ~ **ADNI-Mem** Annual Rate of Change

(B) Network Concordance ~ **ADNI-EF** Annual Rate of Change

FIGURE 6 T-scores of network-wise multivariate regression model assessing for the effect on individual Alzheimer's Disease Neuroimaging Initiative Memory Composite (ADNI-Mem) and Alzheimer's Disease Neuroimaging Initiative Executive Function Composite (ANDI-EF) rate of decline in suspected non-Alzheimer's disease pathologic change (SNAP; N = 139) and Alzheimer's disease (AD) continuum (N = 510), corrected for age, sex, education, apolipoprotein E genotype, and mean W-score of atrophy and hypometabolism. Top panel, ADNI-Mem: Significant networks (colored) include language network in SNAP and primary visual, somatomotor, dorsal attention, language, frontoparietal, auditory, default mode, and orbito-affective networks in AD continuum. There were no significant relationships to ADNI-Mem rate of change for biomarker normal (BN; N = 167). Bottom panel, ADNI-EF: Significant networks (colored) for AD continuum include secondary visual, dorsal attention, frontoparietal, and auditory networks. There were no significant relationships to ADNI-EF rate of change for SNAP or BN

hypothesized to be the result of multiple and/or heterogeneous neuropathological processes that may target diffuse brain regions.[4,5] These diffuse and heterogenous effects are contrasted with a more harmonious neuropathological process driven by Aβ in AD continuum, leading to higher concordance between atrophy and hypometabolism. Thus, our findings support the likelihood that (CSF-defined) SNAP is etiologically heterogenous. This view is supported by research demonstrating that many non-AD neurodegenerative pathologies are common in the elderly, with α-synucleinopathies, non-AD tauopathies, TDP-43 proteinopathy, and vascular lesions present in up to 50% of

samples.[42] Given that SNAP in the present study showed elevated CSF Aβ (indicating less Aβ pathology) compared to both AD continuum and BN (P<.01; Table 1), it is unlikely that SNAP represent individuals on the threshold of amyloid positivity, as has been previously suggested.[43] Given the heterogeneity of the underlying clinicopathological profile of SNAP, it is possible the current sample reflects a limited degree of true "Non-AD [neurodegenerative] pathology." However, sufficient noise from diffuse sources of neurodegeneration may also have reduced concordance of atrophy and hypometabolism across several networks.

We further examined the heterogeneity in the A/T/N groups by comparing cognitively "unimpaired" (MMSE> = 26) and "impaired" (MMSE<26) participants. Compared to BN unimpaired, unimpaired AD continuum showed greater concordance scores in the secondary visual, dorsal attention, language, frontoparietal, and default mode networks, while 11/12 networks in impaired AD continuum showed higher concordance. In SNAP, the unimpaired showed increased concordance only in the posterior multimodal network, while interestingly the impaired SNAP showed increased concordance across the dorsal attention, language, frontoparietal, default mode, and ventral multimodal networks, in a pattern similar to AD continuum. The association of concordance with cognitive impairment suggests that a synchronous loss of both gray matter structure and metabolism may signal the loss of neuronal capacity that more effectively depletes cognitive reserve and performance than either atrophy or hypometabolism alone.

Finally, we examined relationships of individual network concordance measures to 1-year rates of change in cognitive composites ADNI-Mem and ADNI-EF. For AD continuum, memory decline was associated with increased concordance in the dorsal attention, language, frontoparietal, and default mode networks at baseline, and declines in executive functioning were associated with increased concordance in the secondary visual, somatomotor, language, frontoparietal, and default mode networks. These results are consistent with unimodal studies of atrophy and hypometabolism.[44,45] We also found that the language network showed an association to memory decline in SNAP after accounting for the degree of unimodal atrophy and hypometabolism. Many FTLD syndromes are known to affect the language regions.[46] Further, atrophy of the ventral, anterior, and medial temporal cortices, which are part of the language network, is seen in familial FTLD.[47] Future research should examine whether the increased concordance within the language network represents a potential biomarker of neuropathologic change among SNAP who progress to an FTLD syndrome.

Strengths of our study include the examination of concordance at the level of functional brain networks, motivated by evidence that neurodegenerative diseases target and spread along large-scale brain networks.[10] However, a limitation is that regions of peak concordance may not respect network boundaries.[48] Alternative, data-driven measures of concordance may provide important information, including canonical correlation or parallel independent components analysis.[49]

Another strength of our study is the use of biomarker-defined groupings, according to 2018 National Institute on Aging–Alzheimer's Association framework guidelines.[3] However, limitations do exist in this approach. There are multiple clinical diagnostic entities contained within each group, and whether SNAP represents a distinct biological entity is a matter of debate.[50] Also, definitions of SNAP differ across studies, including using CSF cut-offs,[16] neuroimaging only,[51] or CSF biomarkers combined with neuroimaging.[52] These approaches could result in a high degree of variability in clinical or cognitive severity within each A/T/N group, in particular the AD continuum, as up to approximately one-third of cognitively normal older adults carry AD neuropathologies.[53] In addition to reporting cognitively impaired versus unimpaired, future studies could also examine those who are only amyloid positive (e.g., A+T−N−) as a separate group.

In sum, our findings suggest that network-level measures of concordance could differentiate SNAP and AD continuum from BN, better than unimodal measures of cortical atrophy and ^{18}FDG-PET hypometabolism alone. Our findings on the Aβ-negative SNAP group highlight the importance of abnormal markers of p-tau or neurodegeneration in the prediction of future cognitive change and suggest that a coordinated relationship between neurodegeneration and cognitive decline can occur in individuals without Aβ. Our findings further support the notion that multimodal neuroimaging analyses are essential to studies of structure–function relationships that contribute to clinical outcomes and diagnostic uncertainty along the biomarker spectrum of AD.

CONFLICTS OF INTEREST

The authors declare no conflicts of interest.

REFERENCES

1. Jack CR, Knopman DS, Jagust WJ, et al. Hypothetical model of dynamic biomarkers of the Alzheimer's pathological cascade. *Lancet Neurol*, 2010;9(1):119–28.

2. Seeley WW. Mapping neurodegenerative disease onset and progression. *Cold Spring Harb Perspect Biol*, 2017;9(8):a023622.

3. Jack CR Jr, Bennett DA, Blennow K, et al. NIA-AA research framework: toward a biological definition of Alzheimer's disease. *Alzheimers Dement*, 2018;14(4):535–562.

4. Caroli A, Prestia A, Galluzzi S, et al. Mild cognitive impairment with suspected nonamyloid pathology (SNAP): prediction of progression. *Neurology*, 2015;84(5):508–515.

5. Schreiber S, Schreiber F, Lockhart SN, et al. Alzheimer disease signature neurodegeneration and apoe genotype in mild cognitive impairment with suspected non–Alzheimer disease pathophysiology. *JAMA Neurol*, 2017;74(6):650–659.

6. Lorenzi M, Simpson IJ, Mendelson AF, et al. Multimodal image analysis in Alzheimer's disease via statistical modelling of non-local intensity correlations. *Sci Rep*, 2016;6(1):1–8.

7. Vos SJB, Gordon BA, Su Y, et al. NIA-AA staging of preclinical Alzheimer disease: discordance and concordance of CSF and imaging biomarkers. *Neurobiol Aging*, 2016;44:1–8.

8. Bejanin A, La Joie R, Landeau B, et al. Distinct interplay between atrophy and hypometabolism in Alzheimer's versus semantic dementia. *Cereb Cortex*, 2019;29(5):1889-1899.

9. Whitwell JL, Graff-Radford J, Tosakulwong N, et al. Imaging correlations of tau, amyloid, metabolism, and atrophy in typical and atypical Alzheimer's disease. *Alzheimers Dement*, 2018;14(8):1005–1014.

10. Seeley WW, Crawford RK, Zhou J, Miller BL, Greicius MD. Neurodegenerative diseases target large-scale human brain networks. *Neuron*, 2009;62(1):42–52.

11. Iaccarino L, Tammewar G, Ayakta N, et al. Local and distant relationships between amyloid, tau and neurodegeneration in Alzheimer's disease. *Neuroimage Clin* 2018;17:452–464.

12. La Joie R, Bejanin A, Fagan AM, et al. Associations between [18F]AV1451 tau PET and CSF measures of tau pathology in a clinical sample. *Neurology*, 2018;90(4):e282-e290.

13. Jack CR Jr, Bernstein MA, Fox NC, et al. The Alzheimer's disease neuroimaging initiative (ADNI): MRI methods. *J Magn Reson Imaging*, 2008;27(4):685–691.

14. Mueller SG, Weiner MW, Thal LJ, et al. The Alzheimer's disease neuroimaging initiative. *Neuroimage Clin*, 2005;15(4):869–877.

15. Schindler SE, Sutphen CL, Teunissen C, et al. Upward drift in cerebrospinal fluid amyloid β 42 assay values for more than 10 years. *Alzheimers Dement*, 2018;14(1):62–70.

16. Hansson O, Seibyl J, Stomrud E, et al. CSF biomarkers of Alzheimer's disease concord with amyloid-β PET and predict clinical progression: A study of fully automated immunoassays in BioFINDER and ADNI cohorts. *Alzheimers Dement*, 2018;14(11):1470–1481.

17. Fischl B. FreeSurfer. *Neuroimage*, 2012;62(2):774–781.

18. Lerch JP, Evans AC. Cortical thickness analysis examined through power analysis and a population simulation. *Neuroimage*, 2005;24(1):163–173.

19. Jenkinson M, Bannister P, Brady M, Smith S. Improved optimization for the robust and accurate linear registration and motion correction of brain images. *Neuroimage*, 2002;17(2):825–41.

20. Hagler DJ, Saygin AP, Sereno MI. Smoothing and cluster thresholding for cortical surface-based group analysis of fMRI data. *Neuroimage*, 2006;33(4):1093–103.

21. Chetelat G, Desgranges B, Landeau B, et al. Direct voxel-based comparison between grey matter hypometabolism and atrophy in Alzheimer's disease. *Brain*, 2008;131(1):60–71.

22. Ma Da, Popuri K, Bhalla M, et al. Quantitative assessment of field strength, total intracranial volume, sex, and age effects on the goodness of harmonization for volumetric analysis on the ADNI database. *Hum Brain Mapp*, 2019;40(5):1507–1527.

23. Popuri K, Balachandar R, Alpert K, et al. Development and validation of a novel dementia of Alzheimer's type (DAT) score based on metabolism FDG-PET imaging. *Neuroimage Clin*, 2018;18:802–813.

24. Glasser MF, Coalson TS, Robinson EC, et al. A multi-modal parcellation of human cerebral cortex. *Nature*, 2016;536(7615):171–178.

25. Ji JL, Spronk M, Kulkarni K, Repovš G, Anticevic A, Cole MW. Mapping the human brain's cortical-subcortical functional network organization. *Neuroimage*, 2019;185:35–57.

26. Hughes CP, Berg L, Danziger W, Coben LA, Martin RL. A new clinical scale for the staging of dementia. *Br J Psychiatry*, 1982;140(6):566–572.

27. Mathworks I. *MATLAB and statistics toolbox release 2018a*. Natick (Massachusetts, United States); 2018.

28. Worsley Kj, Taylor J, Carbonell F, et al. SurfStat: A Matlab toolbox for the statistical analysis of univariate and multivariate surface and volumetric data using linear mixed effects models and random field theory. *Neuroimage*, 2009;(47):S102.

29. Mitchell AJ. *The Mini-Mental State Examination (MMSE): Update on its Diagnostic Accuracy and Clinical Utility for Cognitive Disorders, in Cognitive Screening Instruments*. Springer. 2017: 37–48.

30. Crane PK, Carle A, Gibbons LE, et al. Development and assessment of a composite score for memory in the Alzheimer's Disease Neuroimaging Initiative (ADNI). *Brain Imaging Behav*, 2012;6(4):502–516.

31. Gibbons LE, Carle AC, Mackin RS, et al. A composite score for executive functioning, validated in Alzheimer's Disease Neuroimaging Initiative (ADNI) participants with baseline mild cognitive impairment. *Brain Imaging Behav*, 2012;6(4):517–527.

32. Team RC, DC R. *A Language and Environment for Statistical Computing*. Vienna, Austria: R Foundation for Statistical Computing; 2012. URL https://www.R-project.org, 2019.

33. Pinheiro J, Bates D, DebRoy S, Heisterkamp S, Van Willigen B & Maintainer R et al., Package 'nlme'. Linear and nonlinear mixed effects models, version, 2017;3(1).

34. Jack CR Jr., Knopman DS, Jagust WJ, et al. Update on hypothetical model of Alzheimer's disease biomarkers. *Lancet Neurol*, 2013;12(2):207.

35. Mutlu J, Landeau B, Gaubert M, De La Sayette V, Desgranges B, Chételat G. Distinct influence of specific versus global connectivity on the different Alzheimer's disease biomarkers. *Brain*, 2017;140(12):3317–3328.

36. Pascoal TA, Mathotaarachchi S, Mohades S, et al. Amyloid-β and hyperphosphorylated tau synergy drives metabolic decline in preclinical Alzheimer's disease. *Mol Psychiatry*, 2017;22(2):306–311.

37. Raj A, Locastro E, Kuceyeski A, Tosun D, Relkin N, Weiner M. Network diffusion model of progression predicts longitudinal patterns of atrophy and metabolism in Alzheimer's disease. *Cell Rep*, 2015;10(3):359–369.

38. Brown JA, Deng J, Neuhaus J, et al. Patient-tailored, connectivity-based forecasts of spreading brain atrophy. *Neuron*, 2019;104(5):856–868. e5.

39. Buckner RL, Sepulcre J, Talukdar T, et al. Cortical hubs revealed by intrinsic functional connectivity: mapping, assessment of stability, and relation to Alzheimer's disease. *J Neurosci*, 2009;29(6):1860–1873.

40. Mutlu J, Landeau B, Tomadesso C, et al. Connectivity disruption, atrophy, and hypometabolism within posterior cingulate networks in Alzheimer's disease. *Front Neurosci*, 2016;10:582.

41. Chiaravalloti A, Barbagallo G, Martorana A, Castellano AE, Ursini F, Schillaci O. Brain metabolic patterns in patients with suspected non-Alzheimer's pathophysiology (SNAP) and Alzheimer's disease (AD): is [18 F] FDG a specific biomarker in these patients? *Eur J Nucl Med Mol Imaging*, 2019;46(9):1796–1805.

42. Chételat G, Ossenkoppele R, Villemagne VL, et al. Atrophy, hypometabolism and clinical trajectories in patients with amyloid-negative Alzheimer's disease. *Brain*, 2016;139(9):2528–2539.

43. Duara R, Loewenstein DA, Shen Q, et al. Amyloid positron emission tomography with 18F-flutemetamol and structural magnetic resonance imaging in the classification of mild cognitive impairment and Alzheimer's disease. *Alzheimers Dement*, 2013;9(3):295–301.

44. Mosconi L, Pupi A, De Leon MJ. Brain glucose hypometabolism and oxidative stress in preclinical Alzheimer's disease. *Ann NY Acad Sci*, 2008;1147:180.

45. Yun HJ, Kwak K, Lee J-M. Multimodal discrimination of Alzheimer's disease based on regional cortical atrophy and hypometabolism. *PLoS One*, 2015;10(6):e0129250.

46. Mesulam M, Rogalski E, Wieneke C, et al. Neurology of anomia in the semantic variant of primary progressive aphasia. *Brain*, 2009;132(9):2553–2565.

47. Lee SE, Tartaglia MC, Yener G, et al. Neurodegenerative disease phenotypes in carriers of MAPT p.A152T, a risk factor for frontotemporal dementia spectrum disorders and Alzheimer disease. *Alzheimer Dis Assoc Disord*, 2013;27(4):302–9.

48. Bagarinao E, Watanabe H, Maesawa S, et al. Reorganization of brain networks and its association with general cognitive performance over the adult lifespan. *Sci Rep*, 2019;9(1):1–15.

49. Tosun D, Schuff N, Mathis CA, Jagust W, Weiner MW. Spatial patterns of brain amyloid-β burden and atrophy rate associations in mild cognitive impairment. *Brain*, 2011;134(4):1077–1088.

50. Jack CR, Knopman DS, Chételat G, et al. Suspected non-Alzheimer disease pathophysiology—concept and controversy. *Nat Rev Neurol*, 2016;12(2):117–124.

51. Wirth M, Villeneuve S, Haase CM, et al. Associations between Alzheimer disease biomarkers, neurodegeneration, and cognition in cognitively normal older people. *JAMA Neurol*, 2013;70(12):1512–1519.

52. Toledo JB, Weiner MW, Wolk DA, et al. Neuronal injury biomarkers and prognosis in ADNI subjects with normal cognition. *Acta Neuropathol Commun*, 2014;2(1):26.

53. Bennett DA, Schneider JA, Arvanitakis Z, et al. Neuropathology of older persons without cognitive impairment from two community-based studies. *Neurology*, 2006;66(12):1837–1844.

SUPPORTING INFORMATION

Additional supporting information may be found in the online version of the article at the publisher's website.